

# Low Temperature Adsorption Versus Pore Size in Activated Carbons

D. Martins<sup>1</sup>, I. Catarino<sup>1</sup>, D. Lopes<sup>1</sup>, I. Esteves<sup>2</sup>, J.P. Mota<sup>2</sup>, G. Bonfait<sup>1</sup>

<sup>1</sup>CEFITEC Departamento de Física, Faculdade de Ciências e Tecnologia, UNL, 2829-516 Caparica, Portugal

<sup>2</sup>REQUIMTE/CQFB, Departamento de Química, Faculdade de Ciências e Tecnologia, UNL, 2829-516 Caparica, Portugal

## ABSTRACT

Activated carbons have been used for a long time at low temperature for cryogenic applications. The physisorption properties depend on the pore geometry and size: this feature can be used to optimize the carbon structure for a specific application. In this work, we report on the low-temperature adsorption properties of He, H<sub>2</sub>, and N<sub>2</sub>, using three activated carbons: a carbon monolith (sample A), a granular carbon (sample B) and a pelletized carbon (sample C) with different pore size distributions. Adsorption measurements were performed between 0.1 mbar and 1 bar and in the range 10 K to 100 K for He, 15 K to 300 K for H<sub>2</sub>, and 70 K to 300 K for N<sub>2</sub>. The isosteric heat of adsorption was obtained: it increases with decreasing pore diameter, as expected from the enhanced solid-fluid interaction potential in smaller pores. The characteristic curves,  $P(T)$  at constant loading, were compared to help choose the correct porosity that meets the requirements (pressure, temperature) of a specific application.

## INTRODUCTION

Activated carbons are widely used in the integration of cryogenic devices<sup>1,2</sup> for their adsorption properties. Extensive adsorption data can be found while aiming the optimization of compressors.<sup>3</sup> While extending their pumping applications to different charcoals and/or gases, a lack of available adsorption data was found for subatmospheric pressure and low temperature: Higher pressure with  $T > 77$  K data found in Chan<sup>4</sup> were extrapolated to predict the behavior of sorption actuator in thermal switches.<sup>5-8</sup>

A volumetric measurement bench was built and validated which allowed us to systematically measure the adsorption characteristics of chosen gas-charcoal pairs. Nitrogen and mercury porosimetry facilities were used for characterization of the charcoals.

This communication presents the preliminary results on three different charcoals which adsorbed three different gases: helium, hydrogen and nitrogen. Charcoals were chosen upon different precursors and forms to measure the influence of porosity. Characterization of the charcoal's porosity is presented and correlated to the isosteric heat of adsorption. Pressure drop during cool-down for fixed amounts of charcoal/gas is presented. The analysis helped to choose a charcoal for some applications. Some selected adsorption isotherms are presented as well.

## METHODS

Three samples of charcoals were studied, their description are shown in Table 1: sample A is a machinable monolith while samples B and C are granules and pellets, respectively.

Characterization analysis of the apparent surface area was performed using the Brunauer-Emmett-Teller (BET) equation and nitrogen isothermal data at 77 K obtained using a commercial *Coulter Omnisorb 610*® instrumentation. The Horvath-Kawazoe (HK) method for micropore assessment was also performed on the same data. Mercury intrusion using *Carlo Eber Porosimeter 400*® allowed assessment of mesopore and macropore determination.

Variable temperature adsorption data were collected by a home made volumetric measurement bench, previously validated.<sup>9</sup> The low temperature cell, filled with the adsorbent, is thermalized to the cold finger of a Gifford-McMahon (GM) cryocooler and is connected by a capillary tube to a calibrated volume at room temperature. The pressure in the system is measured at room temperature using a capacitive sensors. The experiment starts by filling the calibrated volume at a determined pressure (filling pressure) that determines the total amount of gas used in the experimental run. This volume is then opened to the cell and the cell is cooled down, its temperature being controlled. Once equilibrium is reached, temperature and pressure data are measured and the cell temperature is incremented by  $\Delta T$  depending of the temperature range ( $2.5 \text{ K} < \Delta T < 20 \text{ K}$ ) to obtain a new set of  $(P, T)$  data. Adsorption measurements were performed between 0.1 mbar and 1 bar and in the range 10 – 100 K for He, 15–300 K for  $\text{H}_2$ , and 70–300 K for  $\text{N}_2$ . Different experimental runs start with different filling pressure and then yield to different adsorption conditions at the same stabilization temperatures. An adsorption isotherm collects data at fixed temperature from several runs.

Sample A was machined to fit tightly in the cryogenic cell while samples B and C were ground and compacted inside the cell. All samples occupied the same volume cell ( $5 \text{ cm}^3$ ) although each has a different mass.

## RESULTS

Normalized nitrogen isotherms obtained with the commercial facility at 77 K are shown in Figure 1. Such isotherms can be classified as type I isotherm<sup>10</sup> for all the charcoals, which depicts the formation of a monolayer adsorption in micropores.

**Table 1.** Description of the three charcoals studied.

sample	A	B	C
	monolith, compacted carbon fibers based	granular carbon, coconut shell based	extruded pellets (2mm), coal based

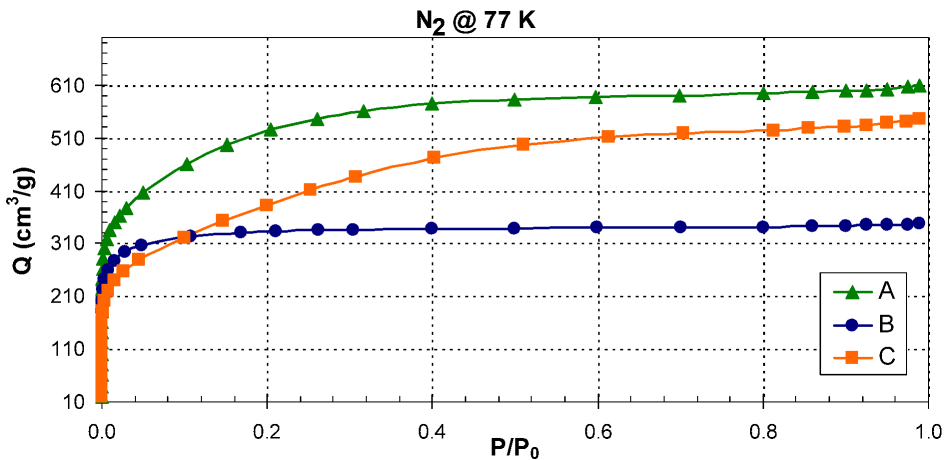


**Figure 1.** Normalized nitrogen isotherms at 77 K, using the commercial facility, identify type I

The volumetric variable temperature method had been previously validated. Nevertheless, Figure 2 shows the overlapping of both adsorption methods with the 77 K isotherm for nitrogen, reinforcing the validity of our homemade facility.

Table 2 presents the porosity characterization of the charcoals which were studied. Sample A presents the highest total pore volume and BET surface area. Sample B has the lowest total pore volume and BET area, but is more microporous (< 6 Å, “narrow micropore”) than sample C; the latter presents an intermediate total pore volume and BET area, exhibiting a significant porosity in the mesopore range.

Although not characteristic of a general sorbate-sorbent system, an easy way to visualize and compare the adsorption capability of the charcoals is by plotting the equilibrium pressure of the system (cold charcoal + room temperature calibrated volume) as a function of the temperature. Figures 3, 4 and 5 show some of these results for different charcoals and different gases. For each gas, the total sorbate amount is kept fixed by using the same initial ambient filling pressure in the same calibrated volume. Charcoal cell volume is also fixed. Analysis of Figures 3 and 5 shows evidence that the charcoal A produces a faster pressure drop than C for both helium and nitrogen. Indeed the monolithic charcoal has the higher surface area, which is no surprise for its higher sorption power. Nevertheless, charcoal B has a lower total surface area than charcoal C, but shows higher sorption effect than C (figure 4). The fact that charcoal B has a much higher narrow micropore volume than charcoal C explains its higher sorption effect for all three gases.

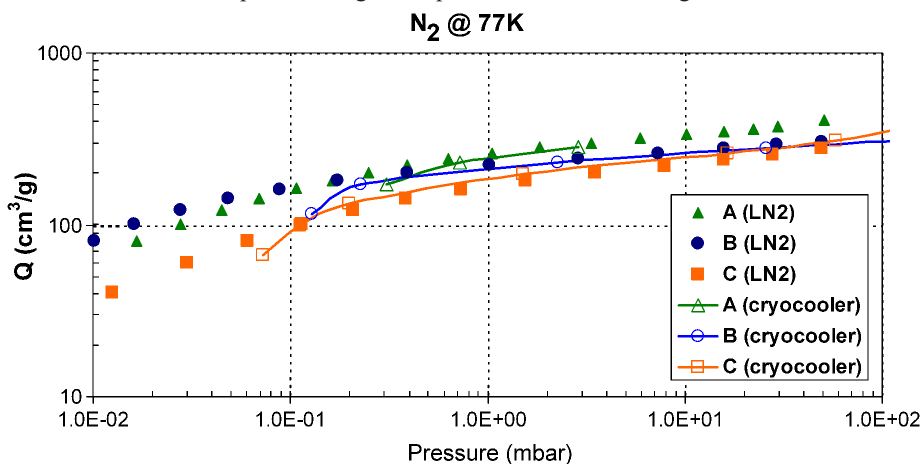


**Figure 2.** Results from commercial (LN2) and home-made (cryocooler) facilities for the adsorption isotherms of nitrogen at 77 K. The agreement between these two types of results helped further validation of our experimental set-up.

**Table 2.** Porosity characterization of the three charcoals studied.

	sample	A	B	C
<b>N2 77K</b>				
BET surface area (m <sup>2</sup> /g)		1740	1077	1355
BET avg pore diameter (Å)		21.71	19.95	24.98
HK total pore volume (cm <sup>3</sup> /g; <200 Å)		0.944	0.537	0.846
HK micropore volume (cm <sup>3</sup> /g; <20 Å)		0.768	0.511	0.544
HK narrow micropore volume (cm <sup>3</sup> /g; <6 Å)		0.282	0.281	0.125
HK broad micropore volume (cm <sup>3</sup> /g; 6-20 Å)		0.486	0.229	0.419
<b>Hg porosimetry</b>				
total pore volume (cm <sup>3</sup> /g; 66-10 <sup>5</sup> Å)		0.469	0.221	0.751
mesopore volume (cm <sup>3</sup> /g; 66-500 Å)		0.101	0.054	0.266
macropore volume (cm <sup>3</sup> /g; 500-10 <sup>5</sup> Å)		0.368	0.167	0.485

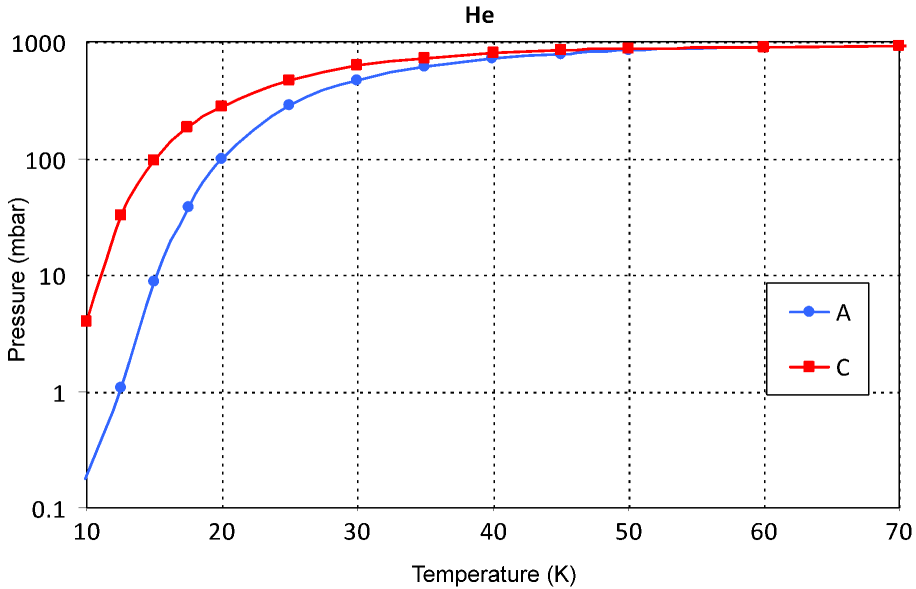


**Figure 3.** "Sorption effect" (pressure versus temperature) for two charcoals under the same amount of helium, same charcoal volume.

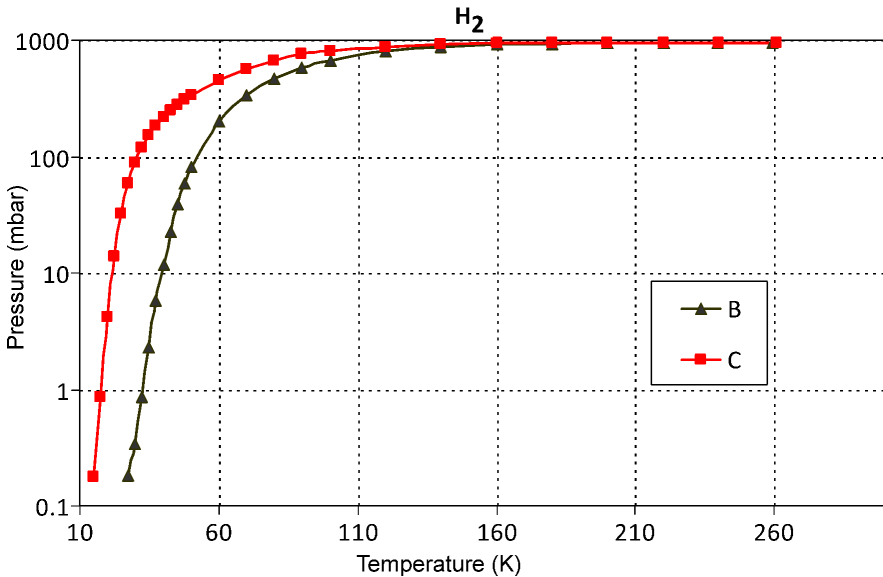


**Figure 4.** "Sorption effect" (pressure versus temperature) for two charcoals under the same amount of hydrogen, same charcoal volume.

From the helium adsorption data plotted in Figure 3, the choice of charcoal A results in an equilibrium pressure lower by more than an order of magnitude for  $T \lesssim 20$  K when compared to charcoal C (for the same total amount of gas and charcoal volume). Such results can be applied to a gas-gap heat switch using helium as the conducting gas<sup>11</sup> and a sorption pump actuator. In such a case, the OFF state (corresponding to a low pressure in the switch) cannot be kept for a charcoal temperature above  $\sim 15$  K. Figure 3 shows that the same low pressure for sample A can be obtained

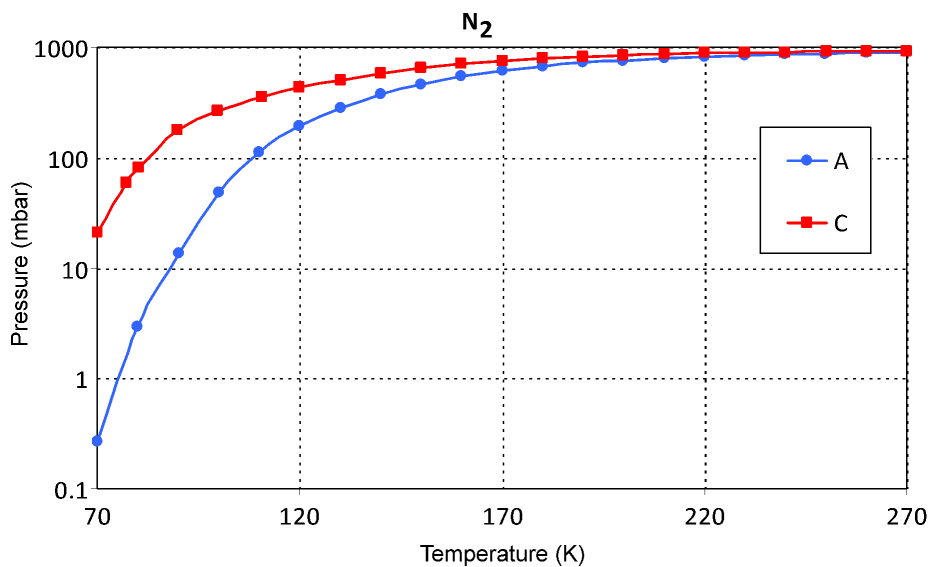


**Figure 5.** “Sorptions effect” (pressure versus temperature) for two charcoals under the same amount of nitrogen, same charcoal volume.

for sample C with a  $\approx +5$  K shift in the charcoal’s temperature. Assuming that this shift remains in this temperature range for lower pressure, this indicates that the OFF state temperature could be tailored within at least 5 K by the correct choice of adsorbent. Further investigation is in progress on this issue.

With  $H_2$ , a gain of two orders of magnitude (Figure 4) in the equilibrium pressure can be obtained below 30 K by properly choosing the charcoal. Similar evidence is shown for  $N_2$  (Figure 5) for  $T < 80$  K. As a matter of fact, the current study on adsorption is being taken into account for customization of gas-gap heat switches under development in our laboratory.<sup>8</sup>

The amount of adsorbed gas per amount of sorbent, commonly called the charge ( $Q$ ), is calculated from known volumes and measured pressures. The adsorption data are more conveniently represented by a relation of two of the state variables  $P$ ,  $Q$  and  $T$ , while keeping the third one constant as in the case of an adsorption isotherm. Some adsorption isotherms for all three charcoal samples are presented, for helium in Figure 6, for nitrogen in Figure 7. Charge  $Q$  is presented in gram of gas per gram of charcoal. Sample A overlaps sample B in all studied cases for the most part.

Actually, charcoals A and B display similar sorptions effects for all three gases. Their total surface areas differ by more than 60% but their narrow micropore ( $< 6 \text{ \AA}$ ) volumes are coincident. This micropore volume seems to be a determining parameter for the observed adsorptions.

The highest helium adsorption is normally related to the highest BET surface.<sup>3</sup> Such is not the case in our experiments, since sample C presents higher BET surface than sample A but a poorer adsorption capability. As already mentioned, the volume of the smaller narrow pores seems to be the determinant geometrical factor as pointed out in Panella’s work.<sup>12</sup>

Data with the same charge ( $Q$ ) are called isosteric. Isosteric data are interpolated from the isotherm data. At low charges  $\ln(P)$  is proportional to  $1/T$  and isosteric heat of adsorption can be calculated using the Clausius-Clapeyron law and the isosteric experimental curves:

$$\Delta h(Q) = - \frac{d \ln(P)}{d(1/T)} \cdot R \tag{1}$$

The heat of adsorption is a function of the adsorbed amount of gas per amount of charcoal. Table 3 presents the isosteric heats of adsorption obtained at low charges. Such energy should

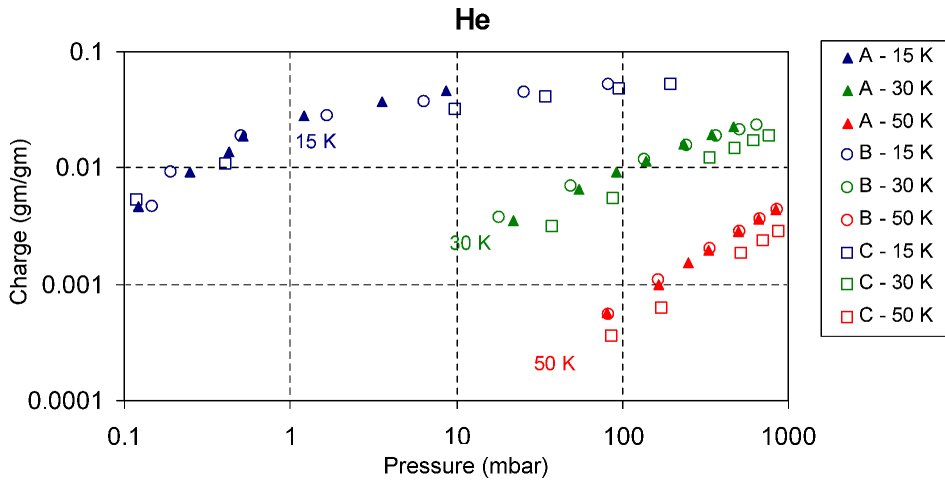


Figure 6. Three selected adsorption isotherms for the gas helium on the three charcoal samples.

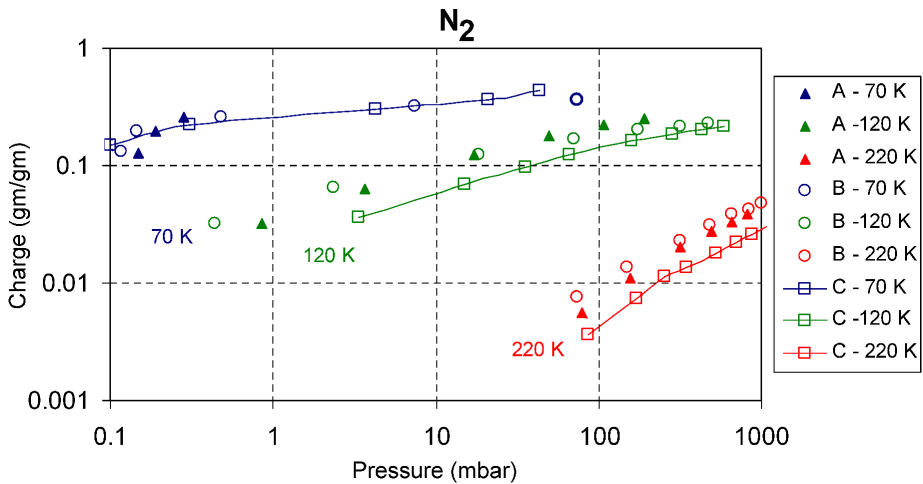


Figure 7. Three selected adsorption isotherms for the gas nitrogen on the three charcoal samples.

Table 3. Experimental heat of adsorption for each pair of gas - charcoal studied.

sample	A	B	C
isosteric heat of adsorption (KJ/mol)			
He	2.3	2.5	2.2
H <sub>2</sub>	n.a.	7.6	6.6
N <sub>2</sub>	14	16	13.8

increase for higher microporosity as expected from the enhanced solid-fluid interaction potential in smaller pores. Sample B exhibits the highest adsorption energy, which is related to its high narrow microporosity (Table 2). Comparable values of 6 kJ/mol could be found in Chan<sup>4</sup> for the heat of adsorption of hydrogen on charcoal, and about 10 kJ/mol for nitrogen.<sup>4</sup>

## CONCLUSIONS

Three different charcoals were characterized for their cryogenic sorption properties with helium, hydrogen and nitrogen at subatmospheric pressures. Pore analysis of the charcoals allowed the assignment of the microporosity as a determinant parameter at their sorption characteristics. Sorption effect plots presented may be found helpful when choosing a charcoal as a pump in a cryogenic integration component. Selected adsorption isotherms were presented for all the gases and charcoals. Sorption studies of similar materials are still being studied. The current results are being used to optimize gas-gap heat switches with cryopump actuators.

## ACKNOWLEDGMENT

This work was partially supported Fundação para a Ciência e Tecnologia (PTDC/EME-MFE/66533 /2006). DM and DL acknowledge the same institution for granting.

## REFERENCES

1. Duband, L., Collaudin, B., "Sorption Coolers Development at CEA-SBT," *Cryogenics*, Vol. 39, Issue: 8, August 1999, pp. 659-663.
2. Doornink, D.J., Burger, J.F., ter Brake, H.J.M., "Sorption cooling: A valid extension to passive cooling," *Cryogenics*, Vol. 48, Issues: 5-6, May-June 2008, pp. 274-9.
3. Lozano-Castelló, D., Jordá-Beneyto, M., Cazorla-Amorós, D., Linares-Solano, A., Burger, J.F, ter Brake, H.J.M., Holland, H.J., "Characteristics of an activated carbon monolith for a helium adsorption compressor," *Carbon*, vol. 48, (2010), pp. 123-31.
4. Chan, C.K., Tward, E., and Boudaie, K.I., "Adsorption isotherms and heats of adsorption of hydrogen, neon and nitrogen on activated charcoal," *Cryogenics*, Vol. 24, Issue: 9, September 1984, pp. 451-9.
5. Catarino, I., Afonso, J., Martins, D., Duband, L., Bonfait, G., "Gas gap thermal switches using neon or hydrogen and sorption pump," *Vacuum*, vol. 83, (2009), pp. 1270-3.
6. Catarino, I., Bonfait, G., Duband, L., "Neon Gas Gap Heat Switch," *Cryogenics*, Vol. 48, Issues: 1-2, January-February 2008, pp. 17-25.
7. Catarino, I., Duband, L., Bonfait, G., "Hydrogen and Neon Gas-Gap Heat Switch," *Cryocoolers 15*, ICC Press, Boulder, CO (2009), pp. 553-9.
8. Martins, D., Catarino, I., Schoeder, U., Ricardo, J., Patricio, R., Duband, L., Bonfait, G., "Customizable Gas-Gap Heat Switch," *Adv. in Cryogenic Engineering*, Vol. 55, Amer. Institute of Physics, Melville, NY (2010), pp. 1682-1690.
9. Lopes, D., "Construction and characterization of a system for cryosorption studies," Master's Thesis, UNL, Lisboa. (2008).
10. F. Rouquerol, J. Rouquerol & K. Sing, *Adsorption by Powders and Porous Solids*, Academic Press, (1999).
11. Duband, L." A Thermal Switch for use at Liquid Helium Temperature in Space Borne Cryogenic Systems," *Cryocoolers 8*, Plenum Press, New York (1995), pp. 731-741.
12. Panella, B., Hirscher, M., Roth, S., "Hydrogen adsorption in different carbon nanostructures," *Carbon*, Vol. 43, (2005), pp. 2209-14.

